

THE GEOMETRY OF ZERO-DETERMINANT STRATEGIES

XINGRU CHEN^{1,2}, LONG WANG³, AND FENG FU^{2,4}

¹*School of Sciences, Beijing University of Posts and Telecommunications, Beijing 100876, China*

²*Department of Mathematics, Dartmouth College, Hanover, NH 03755, USA*

³*Center for Systems and Control, Peking University, Beijing 100871, China*

⁴*Department of Biomedical Data Science, Geisel School of Medicine at Dartmouth, Lebanon, NH 03756, USA*

ABSTRACT

The advent of Zero-Determinant (ZD) strategies has reshaped the study of reciprocity and cooperation in the iterated Prisoner's Dilemma games. The ramification of ZD strategies has been demonstrated through their ability to unilaterally enforce a linear relationship between their own average payoff and that of their co-player. Common practice conveniently represents this relationship by a straight line in the parametric plot of pairwise payoffs. Yet little attention has been paid to studying the actual geometry of the strategy space of all admissible ZD strategies. Here, our work offers intuitive geometric relationships between different classes of ZD strategies as well as nontrivial geometric interpretations of their specific parameterizations. Adaptive dynamics of ZD strategies further reveals the unforeseen connection between general ZD strategies and the so-called equalizers that can set any co-player's payoff to a fixed value. We show that the class of equalizers forming a hyperplane is the critical equilibrium manifold, only part of which is stable. The same hyperplane is also a separatrix of the cooperation-enhancing region where the optimum response is to increase cooperation for each of the four payoff outcomes. Our results shed light on the simple but elegant geometry of ZD strategies that is previously overlooked.

1. INTRODUCTION

The evolution of cooperation is one of the long-standing conundrums facing researchers from diverse fields [1]. Over the past decades, a number of seminal contributions have been made to improve our understanding of cooperation [2]. Among

E-mail address: xingrucz@gmail.com, longwang@pku.edu.cn, fufeng@gmail.com.

others, cooperation can prevail under reciprocal altruism [3], which means “you scratch my back and I will scratch yours.” As a repeated two-player game, Iterated Prisoner’s Dilemma games (IPD) have been the paradigm for studying direct reciprocity and cooperation [4, 5, 6, 7, 8, 9, 10]. In particular, the famous Axelrod’s tournament has ushered in an era of studying powerful IPD strategies using computer simulations in combination with analytical approaches [11, 12].

A plethora of memory- n strategies including deterministic strategies and their stochastic counterparts have been thoroughly investigated [8, 13]. IPD strategies can be as sophisticated as possible, such as finite automata [14], lookup table-based strategies [15], or strategies that are optimized by using techniques like neural networks or swarm particle intelligence [16]. On the other hand, winning IPD strategies can be surprisingly simple but powerful. The prominent Tit-for-Tat (TFT), for example, is such a “fair-minded” strategy that is found to be the backbone of direct reciprocity [6]. In the original version, TFT responds with full cooperation after co-player’s cooperative move but always retaliates with full defection after co-player’s defection. Variants of TFT, often called “compliers” [17], include the so-called generous TFT (GTFT) [7] which forgives co-player’s defection with a certain probability. These special strategies can be part of a larger class of reactive strategies that condition their responses on their co-player’s behavioral choice (C vs D) [7, 18]. The notion of reactive strategies has enabled analytical insights into the evolution of reciprocity and cooperation in the IPD games [19].

Memory-one IPD strategies are further specified by the probability to cooperate for the initial move and the probability to cooperate conditioned on each of the four possible payoff outcomes in a single round, denoted by $[q_1, q_2, q_3, q_4]$. The ordered labels 1, 2, 3, and 4, respectively, refer to the payoff outcome R from the pair of strategy choices, (C, C) , S from (C, D) , T from (D, C) , and P from (D, D) , as described from the focal row player’s perspective via the payoff matrix

$$(1) \quad \begin{array}{cc} & \begin{array}{cc} C & D \end{array} \\ \begin{array}{c} C \\ D \end{array} & \left(\begin{array}{cc} R & S \\ T & P \end{array} \right). \end{array}$$

For Prisoner’s Dilemma (PD), we have $T > R > P > S$. Conventional PD games also assume $2R > T + S > 2P$, that is, mutual cooperation is better than unilateral cooperation better than mutual defection.

From the perspective of evolution, another strategy known as Win-Stay Lose-Shift (WSLS) stands out later [7]. As for payoff control and manipulation, the discovery of equalizers is worthy of note [20]. The authors describe such a simple strategy, up to a properly chosen normalization factor ϕ , $[1 - \phi(R - O), 1 - \phi(T - O), \phi(O - S), \phi(O - P)]$ that is able to set any co-player’s average payoff O to be the exact same amount between P and R . Using an elegant approach of linear algebra [21], Press and

Dyson further show that the so-called Zero-Determinant (ZD) strategies are able to unilaterally enforce a linear relationship between its average payoff s_X and that of the co-player's s_Y , $s_X - O = \chi(s_Y - O)$, where O is the baseline payoff, and χ is the extortion factor. Thus, the class of equalizers becomes a limiting subset of ZD strategies as $\chi \rightarrow \infty$ (that is, to unilaterally set co-player Y 's average payoff s_Y to be O). ZD strategies can be categorized by their intended level of generosity O [22]. The class with $O = P$ and $\chi > 1$ is often called extortionate ZD since these players can always ensure their advantage with an unfair surplus as $s_X - P = \chi(s_Y - P) \geq 0$ for conventional PD games. The class with $O = R$ and $\chi > 1$ is called generous ZD, ensuring that their own average payoff is never greater than the co-player's as $s_X - R = \chi(s_Y - R) \leq 0$.

Efforts on various extensions to ZD strategies have been proven fruitful [23, 24, 25, 26], including but not limited to multi-person games [27, 28, 29, 30], noises or errors [31, 32], and finitely repeated games [33]. The evolution of ZD strategies has been studied in finite populations [17, 34] as well as in structured populations [35]. The overall insight is that extortionate ZD strategies are powerful yet not evolutionarily stable in the sense that they will neutralize each other's advantage unless they adapt to be generous [36, 37, 38, 39]. Nevertheless, they can be the catalysts for the evolution of cooperation that pave the way for the emergence of cooperation (TFT, generous TFT, or more generally, generous ZD). Noteworthy, the dominance and optimality of ZD strategies depend on the underlying payoff structure, which is determined by the sign of $T + S - 2P$ [40]. It is found that a seemingly formidable ZD strategy can actually be outperformed, for example, by WSLs if $T + S < 2P$ and that when against fixed unbending strategies, the best response of ZD players is to offer a fair split by letting $\chi \rightarrow 1$ [40].

Let us now turn to the superset of ZD strategies, which is a collection of memory-one strategies $[q_1, q_2, q_3, q_4]$ with three free parameters (O, χ, ϕ) :

$$(2) \quad \begin{aligned} q_1 &= 1 - \phi(R - O)(\chi - 1), \\ q_2 &= 1 - \phi[(T - O)\chi + (O - S)], \\ q_3 &= \phi[(O - S)\chi + (T - O)], \\ q_4 &= \phi(O - P)(\chi - 1). \end{aligned}$$

For q_i 's must be within $[0, 1]$, the admissible ranges of (O, χ, ϕ) are given by

$$\left\{ \begin{array}{l} P \leq O \leq R, \\ 1 \leq \chi < \infty, \\ 0 \leq \phi \leq \min\left\{\frac{1}{(O-S)\chi+(T-O)}, \frac{1}{(T-O)\chi+(O-S)}\right\}, \end{array} \right.$$

or

$$\left\{ \begin{array}{l} P \leq O \leq R, \\ -\infty \leq \chi \leq \min\{-\frac{O-S}{T-O}, -\frac{T-O}{O-S}\} \leq -1, \\ \max\{\frac{1}{(O-S)\chi+(T-O)}, \frac{1}{(T-O)\chi+(O-S)}\} \leq \phi \leq 0. \end{array} \right.$$

Geometrically, the family of memory-one ZD strategies formally expressed by a 4-dimensional tuple, the quadruple $[0, 1]^4$, is located on a 3-dimensional hyperplane. Without loss of generality, it can be represented by:

$$(3) \quad q_4 = \frac{-(T + S - 2P)q_1 + (R - P)(q_2 + q_3) + T + S - R - P}{2R - T - S}.$$

Prior work has almost exclusively focused on the resulting linear payoff relationship explicitly only with two parameters $s_X - O = \chi(s_Y - O)$, assuming that player X uses a ZD strategy regardless of player Y's chosen strategy. While the ramification of ZD strategies can be conveniently visualized as a straight line in the parametric plot of (s_X, s_Y) , with the slope $1/\chi$ and the invariant point (O, O) , the actual geometry of ZD strategies is paid little attention. Having said so, the present work will shed new light on the elegance of ZD strategies in relation to their parameterizations (O, χ, ϕ) from the previously overlooked perspective of geometry.

2. RESULTS

In this work, we will focus on the geometry of (q_1, q_2, q_3) in the cube $[0, 1]^3$ for specific choices of (O, χ, ϕ) . Unless noted otherwise, we use the correspondence of Cartesian coordinates (x, y, z) with respect to the ordered triplet (q_1, q_2, q_3) . There exists a one-to-one mapping, at least in the small neighborhood of a given ZD strategy, between (q_1, q_2, q_3) and (O, χ, ϕ) except for $\phi = 0$ or $\chi = 1$, since the determinant of the Jacobian is

$$(4) \quad \left| \frac{\partial(q_1, q_2, q_3)}{\partial(O, \chi, \phi)} \right| = (T - S)(2R - T - S)\phi^2(\chi - 1).$$

For $\phi = 0$, the corresponding subset of ZD strategies regardless of the choice of (O, χ) degenerates into a point D $(1, 1, 0)$ (Fig. 1). Meanwhile, for $\chi = 1$, the corresponding subset of ZD strategies regardless of the choice of O forms a line DA connecting $(1, 0, 1)$ and $(1, 1, 0)$ (Figs. 1a - 1c). This line is the common limit subset shared by all ZD strategies as $\chi \rightarrow 1$.

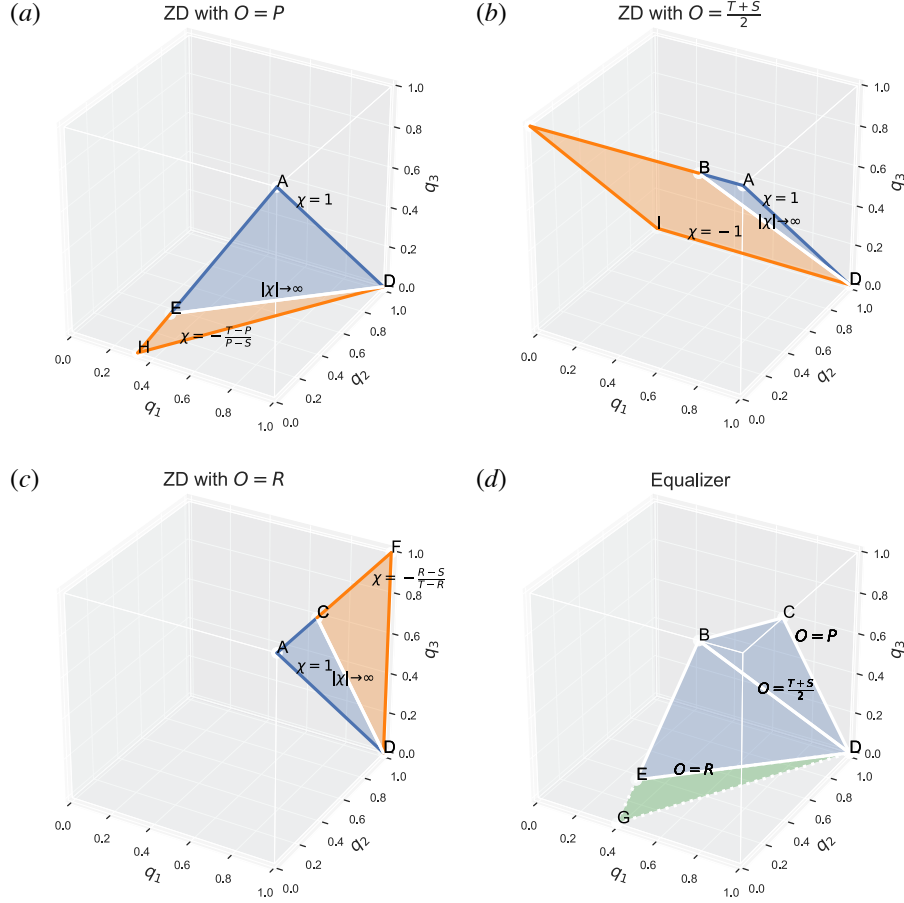


FIGURE 1. Geometry of ZD strategies. Any ZD strategy $[q_1, q_2, q_3, q_4]$ can be visualized in the cube $[0, 1]^3$ for the ordered triplet (q_1, q_2, q_3) using the fact that q_4 is linearly dependent on $q_1, q_2,$ and q_3 , as shown in Eq. (3). (a), (b), and (c) show that ZD strategies with the same baseline payoff O are on the same plane, respectively, for $O = P$, $(T + S)/2$, and R . (d) shows that all equalizer strategies are located on the same plane, indicated by BCDE, and the dashed triangle DEG indicates equalizer strategies that are inadmissible. The lines DE and DB and DC, also highlighted in (a) - (c), present equalizer strategies that are able to fix their co-player's average payoff to be P , $(T + S)/2$, and R , respectively. On the other hand, ZD strategies with different O share the line DA as their common limit for $\chi \rightarrow 1$. When increasing O , the plane formed by ZD strategies with the same O in effect rotates around the axis DA. All ZD strategies sharing the same O and χ are on the same line; for a fixed O , the corresponding line approaches the limit of equalizer monotonically from both directions as χ tends to $+\infty$ from 1 or to $-\infty$ from $\min\{- (O - S)/(T - O), -(T - O)/(O - S)\}$, namely, from DA to DE and from DH to DE in (a), from DA to DB and from DI to DB in (b), and from DA to DC and from DF to DC in (c). For all figures in the paper, we consider the conventional payoff matrix $[R, S, T, P] = [3, 0, 5, 1]$.

For ZD strategies not in the line DA, their (O, χ, ϕ) can be uniquely determined by (q_1, q_2, q_3) :

$$(5) \quad \begin{aligned} O &= \frac{(T+S)q_1 - R(q_2 + q_3) + R - T - S}{2q_1 - q_2 - q_3 - 1}, \\ \chi &= \frac{(T-S)q_1 - (T-R)q_2 - (R-S)q_3 - (R-S)}{-(T-S)q_1 + (R-S)q_2 + (T-R)q_3 + T - R}, \\ \phi &= \frac{(T-S)q_1 - (R-S)q_2 - (T-R)q_3 - (T-R)}{(T-S)(2R - T - S)}. \end{aligned}$$

For ZD strategies with the same O , they all together form a 2-dimensional plane (Figs. 1a - 1c), given by

$$(6) \quad q_3 = \frac{(T+S-2O)q_1 - (R-O)q_2 + R + O - T - S}{R - O}.$$

The normal vector of this “ O -fixed plane” is $\vec{n} = [T+S-2O, -(R-O), -(R-O)]$. For instance, for baseline payoff $O = P$, the normal vector of this plane is $[T+S-2P, -(R-P), -(R-P)]$ and for $O = R$, the normal vector is $[2R-T-S, 0, 0]$, or simply $[1, 0, 0]$.

Of particular interest, the “equalizer” subset of ZD strategies (obtained by letting $|\chi| \rightarrow +\infty$) forms another plane (Fig. 1d), which can be written as

$$(7) \quad q_3 = \frac{(T-S)q_1 - (R-S)q_2 - (T-R)}{T-R}.$$

We note that the equation above is exactly equivalent to the denominator of the expression of χ as a function of (q_1, q_2, q_3) given in Eq. (5). This plane of equalizer intersects with the plane of ZD strategies with fixed O , and the intersection line fixes any co-player’s payoff to the same level O (Fig. 1d).

For any given O , all of the corresponding ZD strategies contain the line DA connecting $(1, 1, 0)$ and $(1, 0, 1)$. In other words, the resulting plane formed by ZD strategies, while varying O from P to R , rotates with a common axis DA which is the line connecting $(1, 1, 0)$ and $(1, 0, 1)$. This unprecedented geometry of ZD strategies can also be indirectly validated by the fact that the normal vector of the plane $\vec{n} = [T+S-2O, -(R-O), -(R-O)]$ formed by ZD strategies is always orthogonal to the vector $DA = [0, -1, 1]$ for $P \leq O \leq R$.

To further explain the geometrical meaning of the parameters (O, χ, ϕ) , we now turn to specific examples of ZD strategies with $O = P, (T+S)/2, R$, respectively, as illustrated in Fig. 1. For ZD strategies on the same line that passes through any given triplet (q_1, q_2, q_3) and $(1, 1, 0)$ (that is, point D), they all share the same O and χ . For fixed O , all the lines formed by such ZD strategies are on the same plane (Figs. 1a - 1c); when varying χ , the resulting line rotates around $(1, 1, 0)$ towards a direction

that depends on the sign of χ but has the exact same limiting position as $|\chi| \rightarrow +\infty$. For increasing positive χ , the angle between this line and the vector $DA = [0, -1, 1]$ monotonically increases with χ until reaching the limit of the “equalizer” plane. For decreasing negative χ , the line monotonically approaches the same “equalizer” line but from the other direction. In the following, we show this for positive χ values. The case for negative χ can be demonstrated analogously.

The angle θ between the vector $[q_1 - 1, q_2 - 1, q_3]$ and $[0, -1, 1]$ is ϕ -independent and given by

$$(8) \quad \begin{aligned} \cos \theta &= \frac{(q_1 - 1, q_2 - 1, q_3) \cdot (0, -1, 1)}{|(q_1 - 1, q_2 - 1, q_3)| \cdot |(0, -1, 1)|} \\ &= \frac{\sqrt{2}(T - S)(\chi + 1)}{2\{(R - O)^2(\chi - 1)^2 + [(T - O)\chi + O - S]^2 + [(O - S)\chi + T - O]^2\}^{1/2}}. \end{aligned}$$

Its derivative with respect to χ is

$$(9) \quad \frac{d \cos \theta}{d\chi} = -\frac{\sqrt{2}(T - S)(\chi - 1)[6O^2 - 4O(T + R + S) + 2R^2 + (T + S)^2]}{2\{(R - O)^2(\chi - 1)^2 + [(T - O)\chi + O - S]^2 + [(O - S)\chi + T - O]^2\}^{3/2}}.$$

Because

$$(10) \quad f(O) = 6O^2 - 4O(T + R + S) + 2R^2 + (T + S)^2 \geq f\left(\frac{T + R + S}{3}\right) = \frac{(2R - T - S)^2}{3} > 0,$$

we have $d \cos \theta / d\chi < 0$, suggesting that as χ increases, the line formed by ZD with the same O and χ rotates around the point $(1, 1, 0)$ towards the equalizer limit line as $\chi \rightarrow +\infty$. For negative χ , the corresponding line similarly rotates around the point $(1, 1, 0)$ towards the equalizer limit line as $\chi \rightarrow -\infty$.

Further, the equalizer plane separates all admissible ZD strategies into two regions: those above the plane with positive χ values whereas those below the plane with negative χ values (Fig. 2).

Most strikingly, we find the nontrivial emergence of “equalizers” as the equilibrium manifold appearing in the adaptive dynamics of ZD strategies explicitly in the strategy space (p_1, p_2, p_3) (Fig. 3a).

Assuming ZD strategies $\mathbf{p} = [p_1, p_2, p_3, p_4]$ vs $\mathbf{q} = [q_1, q_2, q_3, q_4]$, both satisfying Eq. (3), Press and Dyson show that the average payoff $\pi(\mathbf{p}, \mathbf{q})$ of player using \mathbf{p} can

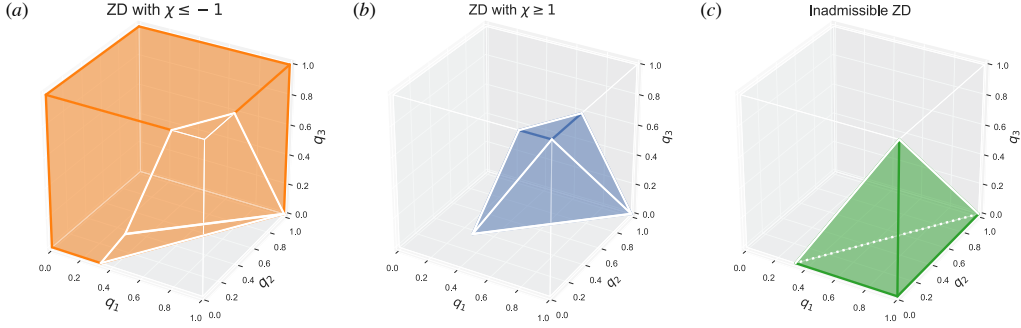


FIGURE 2. Strategy space of admissible ZD strategies. The plane of equalizers separates the space of admissible ZD strategies into two regions: those with negative χ values in (a) and those with positive χ values in (b). The shaded region in (c) below the plane formed by ZD with $O = P$ (more specifically, triangle ADH in Fig. 1) and containing the corner $(1, 0, 0)$ of the cube is inadmissible as ZD strategies.

be calculated as

$$(11) \quad \pi(\mathbf{p}, \mathbf{q}) = \frac{\det \begin{vmatrix} p_1 q_1 - 1 & p_1 - 1 & q_1 - 1 & R \\ p_2 q_3 & p_2 - 1 & q_3 & S \\ p_3 q_2 & p_3 & q_2 - 1 & T \\ p_4 q_4 & p_4 & q_4 & P \end{vmatrix}}{\det \begin{vmatrix} p_1 q_1 - 1 & p_1 - 1 & q_1 - 1 & 1 \\ p_2 q_3 & p_2 - 1 & q_3 & 1 \\ p_3 q_2 & p_3 & q_2 - 1 & 1 \\ p_4 q_4 & p_4 & q_4 & 1 \end{vmatrix}}.$$

The adaptive dynamics of ZD strategies can be obtained by

$$(12) \quad \frac{dq_i}{dt} = \frac{\partial \pi(\mathbf{p}, \mathbf{q})}{\partial p_i} \Big|_{\mathbf{p}=\mathbf{q}}.$$

After a bit of algebra, we get

$$(13) \quad \begin{aligned} \frac{dq_1}{dt} &= \frac{(q_2 + q_3 - 1)[(T - S)q_1 - (R - S)q_2 - (T - R)q_3 - (T - R)]}{(1 - q_2 + q_3)(1 - 2q_1 + q_2 + q_3)^2}, \\ \frac{dq_2}{dt} &= \frac{1 - q_1}{q_2 + q_3 - 1} \cdot \frac{dq_1}{dt}, \\ \frac{dq_3}{dt} &= \frac{dq_2}{dt}. \end{aligned}$$

We see that the selection gradient is zero at the equalizer plane, forming the equilibrium manifold of the corresponding adaptive dynamics (Fig. 3a).

A simple calculation shows that

$$(14) \quad (q_1 - 1)\frac{dq_1}{dt} + (q_2 - 1)\frac{dq_2}{dt} + q_3\frac{dq_3}{dt} = 0.$$

Thus, the direction of the vector field $[dq_1/dt, dq_2/dt, dq_3/dt]$ is orthogonal to the vector $[q_1 - 1, q_2 - 1, q_3]$ that points from $(1, 1, 0)$ to (q_1, q_2, q_3) . As a matter of fact, the vector field is formed by the concentric spheres around the corner $(1, 1, 0)$.

2.1. Stability of the equilibrium manifold. The normal vector of the equalizer plane is $[T - S, -(R - S), -(T - R)]$. Its dot product with the selection gradient $[dq_1/dt, dq_2/dt, dq_3/dt]$ near the equilibrium manifold would be

$$(15) \quad \begin{aligned} & [T - S, -(R - S), -(T - R)] \cdot \left[\frac{dq_1}{dt}, \frac{dq_2}{dt}, \frac{dq_3}{dt} \right] \\ &= \frac{(T - S)(q_1 + q_2 + q_3 - 2)[(T - S)q_1 - (R - S)q_2 - (T - R)q_3 - (T - R)]}{(1 - q_2 + q_3)(1 - 2q_1 + q_2 + q_3)^2}. \end{aligned}$$

The sign of this dot product can be used to determine the local stability of the equilibrium manifold. In particular, the plane $q_1 + q_2 + q_3 - 2 = 0$ intersects with the equalizer plane and divides it into stable and unstable parts (Fig. 3a).

2.2. cooperation-enhancing region. In the full strategy space, the cooperation-enhancing region can be found by requiring $\frac{dq_i}{dt} > 0$ for $i = 1, 2, 3, 4$. Using Eq. (3), we get

$$(16) \quad \begin{aligned} \frac{dq_4}{dt} &= \frac{1}{2R - S - T} \left[-(T + S - 2P)\frac{dq_1}{dt} + (R - P)\left(\frac{dq_2}{dt} + \frac{dq_3}{dt}\right) \right] \\ &= \frac{2(R - P)(1 - q_1) - (T + S - 2P)(q_2 + q_3 - 1)}{(2R - T - S)(q_2 + q_3 - 1)} \cdot \frac{dq_1}{dt}. \end{aligned}$$

We thus obtain the critical plane $2(R - P)(1 - q_1) - (T + S - 2P)(q_2 + q_3 - 1) = 0$ so as to determine the sign of dq_4/dt . This plane is in fact the O -fixed plane (see Eq. (6)) formed by ZD strategies with the specific O value satisfying $(T + S)/2 < O < R$ and

$$(17) \quad \frac{2O - T - S}{R - O} = \frac{2(R - P)}{T + S - 2P}.$$

Hence the cooperation-enhancing region (as shown in Fig. 3b) is given by

$$(18) \quad \begin{aligned} & q_2 + q_3 - 1 > 0, \\ & (T - S)q_1 - (R - S)q_2 - (T - R)q_3 - (T - R) > 0, \\ & 2(R - P)(1 - q_1) - (T + S - 2P)(q_2 + q_3 - 1) > 0. \end{aligned}$$

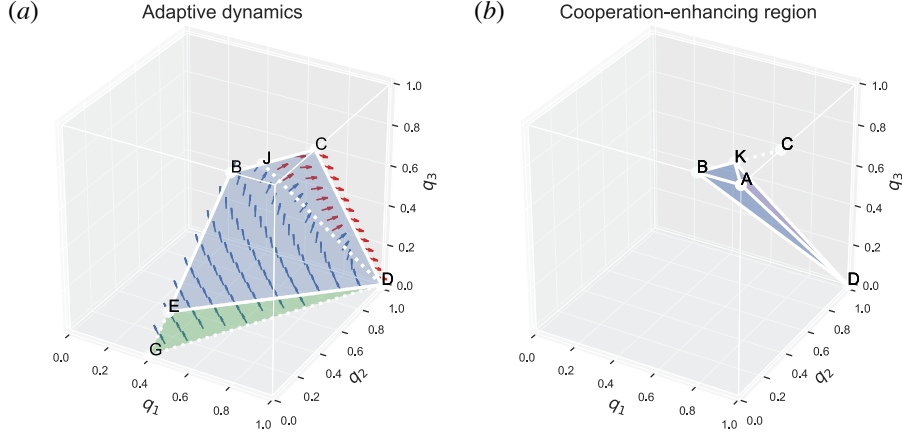


FIGURE 3. Adaptive dynamics of ZD strategies. For clarity, (a) only shows the 3-dimensional vector field plot near the critical equilibrium manifold, which is the plane of equalizer strategies. Part of the equilibrium manifold, indicated by BEDJ, is stable and the remaining part, CDJ, is unstable. Different colors are used to indicate the sign of the dot product in Eq. (15): blue for positive and red for negative. The line DJ is the intersection of the plane $q_1 + q_2 + q_3 - 2 = 0$ and the equalizer plane. The vector field $[dq_1/dt, dq_2/dt, dq_3/dt]$ is orthogonal to the vector $[q_1 - 1, q_2 - 1, q_3]$ that points from $(1, 1, 0)$ towards (q_1, q_2, q_3) . (b) shows the cooperation-enhancing region where dq_i/dt is positive for $i = 1, 2, 3, 4$ in adaptive dynamics. In this region, it is optimal for ZD strategies to increase their probabilities to cooperate invariably, after each of the four outcomes.

2.3. Equal gains from switching: $T + S = R + P$. A necessary condition for reactive strategies to be ZD strategies is that the four payoff values need to satisfy the so-called equal gains from switching: $T + S = R + P$. Under this condition, we may further get $q_1 = q_3$ and $q_2 = q_4$.

By letting $q_1 = q_3$ and $q_2 = q_4$, we obtain $\phi = 1/[(R - S)\chi + T - R]$ and $\phi = 1/[(T - P)\chi + P - S]$, respectively. Moreover, equating these two ϕ values yields

$$(19) \quad \frac{(T + S - R - P)(\chi - 1)}{[(R - S)\chi + T - R][(T - P)\chi + P - S]} = 0.$$

Hence, the payoff condition $T + S = R + P$ is required as desired. To obtain the reactive strategy $[q_1, q_2, q_1, q_2]$ properly from the superset of ZD strategies, we also

need to employ the following combinations of (O, χ) :

$$(20) \quad \begin{aligned} O &= \frac{(T+S)(1-q_1) + R(q_1+q_2-1)}{1-q_1+q_2}, \\ \chi &= \frac{R-S - (T-R)(q_1-q_2)}{(R-S)(q_1-q_2) - (T-R)}. \end{aligned}$$

Under this payoff structure condition, another interesting finding is that unconditional strategies ($q_1 = q_2 = q_3 = q_4$) are ZD strategies with negative χ . Using Eq. (3) and forcing $q_1 = q_2 = q_3$, we get $q_4 = q_1 + (T+S-R-P)/(2R-T-S)$, which leads to the same “equal gains from switching”, $T+S = R+P$, in order for $q_4 = q_1$. The corresponding choice of O, χ, ϕ are now

$$(21) \quad \begin{aligned} O &= (2R-T-S)q_1 + T+S-R, \\ \chi &= -\frac{R-S}{T-R}, \\ \phi &= -\frac{T-R}{(T-S)(2R-T-S)}. \end{aligned}$$

2.4. Fun facts about ZD strategies. The term $2q_1 - q_2 - q_3 - 1$ is the denominator of the expression of O as a function of (q_1, q_2, q_3) in Eq. (5). For all admissible ZD strategies, we actually have

$$(22) \quad 2q_1 - q_2 - q_3 - 1 < 0.$$

Algebraically, using Eq. (2), we get $2q_1 - q_2 - q_3 - 1 = -(2R-T-S)\phi(\chi-1) < 0$ for any admissible parameter choices. The same inequality can also be shown by utilizing the exquisite geometry of ZD strategies. As $O \rightarrow -\infty$, the O -fixed plane approaches the limit $q_3 = 2q_1 - q_2 - 1$, which is further below the plane for $O = P$. Likewise, as $O \rightarrow +\infty$, the O -fixed plane rotates further beyond the plane corresponding to $O = R$ (whose equation is $q_1 = 1$) and approaches the same limit from the other direction. Since a ZD strategy only admits $P \leq O \leq R$, it follows that $q_3 > 2q_1 - q_2 - 1$ for all ZD strategies. Hence we obtain the inequality above as desired.

3. DISCUSSIONS AND CONCLUSION

In this paper, we focus on the payoff structure of conventional PD games satisfying $T+S > 2P$. It is not impossible that in some PD games $T+S < 2P$ holds, that is, the polygon connecting (R, R) , (S, T) , (P, P) , and (T, S) is non-convex in the pairwise payoff plot [40]. Under this circumstance of more adversarial nature, the geometry of Zero-Determinant (ZD) strategies can be studied similarly. It is also worth noting that, for games satisfying “equal gains from switching”, $T+S = R+P$, reactive strategies (including unconditional strategies) become special cases of ZD strategies.

Scrutinizing the geometry of ZD strategies provides useful intuition about and insights into how ZD strategies relate to one another. The parameterization combination (O, χ, ϕ) of ZD strategies determine the admissible range of $\mathbf{q} = [q_1, q_2, q_3, q_4]$ that can be realized. Each subset of ZD strategies with a fixed O value contains a common extreme boundary AD (Figs. 1a - 1c) that is a linear interpolation of TFT ($\mathbf{q} = [1, 0, 1, 0]$) and ‘‘AllC or AllD’’ ($\mathbf{q} = [1, 1, 0, 0]$). The line formed by ZD strategies sharing the same (O, χ) approaches the limit of equalizer strategies, located on the plane BCDE (Fig. 1d), as $\chi \rightarrow +\infty$ or $\chi \rightarrow -\infty$. This equalizer plane in fact separates the strategy space (q_1, q_2, q_3) of admissible ZD strategies into two regions with positive versus negative χ values (Figs. 2a - 2b). We also realize that the region of the cube under the plane expanded by ZD strategies with $O = P$ and containing the corner $(1, 0, 0)$ is inadmissible for any ZD strategies (Fig. 2c).

From the perspective of evolution, it is straightforward to use the adaptive dynamics of ZD strategies to figure out the potential optimal ZD strategies against each other. We find that the common line AD of all ZD strategies with $\chi \rightarrow 1$ emerges as a particular equilibrium. More generally, the plane of equalizers is the non-trivial equilibrium manifold, part of which is stable whereas the remaining part is not (Fig. 3a). The same plane acts as a separatrix of the cooperation-enhancing region that encourages increases in cooperation for each q_i where $i = 1, 2, 3, 4$ (Fig. 3b).

In sum, this paper reveals the non-trivial and elegant geometry of ZD strategies that is previously overlooked. Our present work offers a geometrical interpretation of the ZD parameters (O, χ, ϕ) and particularly the unprecedented geometrical relationships of ZD strategies in the entire strategy space of memory-one IPD strategies with $\mathbf{q} = [q_1, q_2, q_3, q_4]$. Most interestingly, we find that the subset of equalizer strategies forms the critical plane in the strategy space that emerges as the critical equilibrium manifold in the adaptive dynamics of ZD strategies and also as a separatrix of the cooperation-enhancing region. These results highlight the previously unforeseen connection between equalizers and general ZD strategies.

4. APPENDIX

The symbolic coordinates of the points in all the figures are given below. Here, $d_k = (T - P)^2 + (R - P)^2 + (R - S)^2 - 2(P - S)^2$.

$$\begin{aligned}
 \text{A: } & (1, 0, 1) & \text{B: } & \left(\frac{2(T-R)}{T-S}, 0, 1\right) & \text{C: } & \left(1, \frac{2R-T-S}{R-S}, 1\right) \\
 \text{D: } & (1, 1, 0) & \text{E: } & \left(\frac{T-R}{T-P}, 0, \frac{P-S}{T-P}\right) & \text{F: } & (1, 1, 1) \\
 \text{G: } & \left(\frac{T-R}{T-S}, 0, 0\right) & \text{H: } & \left(\frac{T+S-R-P}{T+S-2P}, 0, 0\right) & \text{I: } & (0, 1, 0) \\
 \text{J: } & \left(\frac{2T-R-S}{T+R-2S}, \frac{2R-T-S}{T+R-2S}, 1\right) & \text{K: } & \left(1 - \frac{(T+S-2P)(2R-T-S)}{d_k}, \frac{2(R-P)(2R-T-S)}{d_k}, 1\right)
 \end{aligned}$$

In particular, if we consider the conventional Prisoner’s Dilemma game with payoff matrix $[R, S, T, P] = [3, 0, 5, 1]$, we further get the following specific numbers for all the figures.

$$\begin{aligned}
 \text{B: } & \left(\frac{4}{5}, 0, 1\right) & \text{C: } & \left(1, \frac{1}{3}, 1\right) & \text{E: } & \left(\frac{1}{2}, 0, \frac{1}{4}\right) & \text{G: } & \left(\frac{2}{5}, 0, 0\right) \\
 \text{H: } & \left(\frac{1}{3}, 0, 0\right) & \text{J: } & \left(\frac{7}{8}, \frac{1}{8}, 1\right) & \text{K: } & \left(\frac{8}{9}, \frac{4}{27}, 1\right)
 \end{aligned}$$

4.1. Data availability. All data pertaining to the present work has been included in the paper.

4.2. Code availability. The Python Jupyter notebook that can be used to reproduce results in the paper is available at Github: <https://github.com/fufeng/ZDGeometry>.

REFERENCES

- [1] Robert Axelrod and William D Hamilton. The evolution of cooperation. *Science*, 211(4489):1390–1396, 1981.
- [2] Martin A Nowak. Five rules for the evolution of cooperation. *Science*, 314(5805):1560–1563, 2006.
- [3] Robert L Trivers. The evolution of reciprocal altruism. *The Quarterly review of biology*, 46(1):35–57, 1971.
- [4] Robert Boyd and Jeffrey P Lorberbaum. No pure strategy is evolutionarily stable in the repeated prisoner’s dilemma game. *Nature*, 327(6117):58–59, 1987.
- [5] Martin Nowak et al. An evolutionarily stable strategy may be inaccessible. *Journal of theoretical biology*, 142(2):237–241, 1990.
- [6] Martin A Nowak and Karl Sigmund. Tit for tat in heterogeneous populations. *Nature*, 355(6357):250–253, 1992.
- [7] Martin Nowak and Karl Sigmund. A strategy of win-stay, lose-shift that outperforms tit-for-tat in the prisoner’s dilemma game. *Nature*, 364(6432):56–58, 1993.
- [8] Christoph Hauert and Heinz Georg Schuster. Effects of increasing the number of players and memory size in the iterated prisoner’s dilemma: a numerical approach. *Proceedings of the Royal Society of London. Series B: Biological Sciences*, 264(1381):513–519, 1997.

- [9] Drew Fudenberg and Eric Maskin. The folk theorem in repeated games with discounting or with incomplete information. In *A long-run collaboration on long-run games*, pages 209–230. World Scientific, 2009.
- [10] Te Wu, Feng Fu, and Long Wang. Coevolutionary dynamics of aspiration and strategy in spatial repeated public goods games. *New Journal of Physics*, 20(6):063007, 2018.
- [11] Martin Nowak. Stochastic strategies in the prisoner’s dilemma. *Theoretical population biology*, 38(1):93–112, 1990.
- [12] Robert Axelrod. Launching “the evolution of cooperation”. *Journal of theoretical biology*, 299:21–24, 2012.
- [13] Christian Hilbe, Luis A Martinez-Vaquero, Krishnendu Chatterjee, and Martin A Nowak. Memory- n strategies of direct reciprocity. *Proceedings of the National Academy of Sciences*, 114(18):4715–4720, 2017.
- [14] Ariel Rubinstein. Finite automata play the repeated prisoner’s dilemma. *Journal of economic theory*, 39(1):83–96, 1986.
- [15] Tuomas W Sandholm and Robert H Crites. Multiagent reinforcement learning in the iterated prisoner’s dilemma. *Biosystems*, 37(1-2):147–166, 1996.
- [16] Marc Harper, Vincent Knight, Martin Jones, Georgios Koutsovoulos, Nikoleta E Glynatsi, and Owen Campbell. Reinforcement learning produces dominant strategies for the iterated prisoner’s dilemma. *PLOS One*, 12(12):e0188046, 2017.
- [17] Christian Hilbe, Martin A Nowak, and Karl Sigmund. Evolution of extortion in iterated prisoner’s dilemma games. *Proceedings of the National Academy of Sciences*, 110(17):6913–6918, 2013.
- [18] Seung Ki Baek, Hyeong-Chai Jeong, Christian Hilbe, and Martin A Nowak. Comparing reactive and memory-one strategies of direct reciprocity. *Scientific Reports*, 6(1):1–13, 2016.
- [19] Karl Sigmund. The calculus of selfishness. In *The Calculus of Selfishness*. Princeton University Press, 2010.
- [20] Maarten C Boerlijst, Martin A Nowak, and Karl Sigmund. Equal pay for all prisoners. *The American mathematical monthly*, 104(4):303–305, 1997.
- [21] William H Press and Freeman J Dyson. Iterated prisoner’s dilemma contains strategies that dominate any evolutionary opponent. *Proceedings of the National Academy of Sciences*, 109(26):10409–10413, 2012.
- [22] Alexander J Stewart and Joshua B Plotkin. From extortion to generosity, evolution in the iterated prisoner’s dilemma. *Proceedings of the National Academy of Sciences*, 110(38):15348–15353, 2013.
- [23] Alex McAvoy and Christoph Hauert. Autocratic strategies for iterated games with arbitrary action spaces. *Proceedings of the National Academy of Sciences*, 113(13):3573–3578, 2016.
- [24] Masahiko Ueda. Memory-two zero-determinant strategies in repeated games. *Royal Society open science*, 8(5):202186, 2021.
- [25] Vincent A Knight, Marc Harper, Nikoleta E Glynatsi, and Jonathan Gillard. Recognising and evaluating the effectiveness of extortion in the iterated prisoner’s dilemma. *arXiv preprint arXiv:1904.00973*, 2019.
- [26] Alain Govaert and Ming Cao. Zero-determinant strategies in repeated multiplayer social dilemmas with discounted payoffs. *IEEE Transactions on Automatic Control*, 66(10):4575–4588, 2020.

- [27] Christian Hilbe, Bin Wu, Arne Traulsen, and Martin A Nowak. Cooperation and control in multiplayer social dilemmas. *Proceedings of the National Academy of Sciences*, 111(46):16425–16430, 2014.
- [28] Liming Pan, Dong Hao, Zhihai Rong, and Tao Zhou. Zero-determinant strategies in iterated public goods game. *Scientific reports*, 5(1):1–10, 2015.
- [29] Christian Hilbe, Bin Wu, Arne Traulsen, and Martin A Nowak. Evolutionary performance of zero-determinant strategies in multiplayer games. *Journal of theoretical biology*, 374:115–124, 2015.
- [30] Fang Chen, Te Wu, and Long Wang. Evolutionary dynamics of zero-determinant strategies in repeated multiplayer games. *Journal of Theoretical Biology*, page 111209, 2022.
- [31] Dong Hao, Zhihai Rong, and Tao Zhou. Extortion under uncertainty: Zero-determinant strategies in noisy games. *Physical Review E*, 91(5):052803, 2015.
- [32] Azumi Mamiya and Genki Ichinose. Zero-determinant strategies under observation errors in repeated games. *Physical Review E*, 102(3):032115, 2020.
- [33] Genki Ichinose and Naoki Masuda. Zero-determinant strategies in finitely repeated games. *Journal of theoretical biology*, 438:61–77, 2018.
- [34] Christian Hilbe, Martin A Nowak, and Arne Traulsen. Adaptive dynamics of extortion and compliance. *PLoS One*, 8(11):e77886, 2013.
- [35] Attila Szolnoki and Matjaž Perc. Evolution of extortion in structured populations. *Physical Review E*, 89(2):022804, 2014.
- [36] Christoph Adami and Arend Hintze. Evolutionary instability of zero-determinant strategies demonstrates that winning is not everything. *Nature communications*, 4(1):1–8, 2013.
- [37] Jing Chen and Aleksey Zinger. The robustness of zero-determinant strategies in iterated prisoner’s dilemma games. *Journal of theoretical biology*, 357:46–54, 2014.
- [38] Christian Hilbe, Arne Traulsen, and Karl Sigmund. Partners or rivals? strategies for the iterated prisoner’s dilemma. *Games and economic behavior*, 92:41–52, 2015.
- [39] Ethan Akin. The iterated prisoner’s dilemma: good strategies and their dynamics. *Ergodic Theory, Advances in Dynamical Systems*, pages 77–107, 2016.
- [40] Xingru Chen and Feng Fu. Outlearning extortioners by fair-minded unbending strategies. *arXiv preprint arXiv:2201.04198*, 2022.